

# Controlled transport of solitons and bubbles using external perturbations

J. A. González<sup>1\*</sup>, A. Marcano<sup>1</sup>, B. A. Mello<sup>2</sup>, and L. Trujillo<sup>1†</sup>

<sup>1</sup>*Centro de Física, Instituto Venezolano de Investigaciones Científicas (IVIC),  
A.P. 21827, Caracas 1020-A, Venezuela and*

<sup>2</sup>*IBM Corporation, Thomas I. Watson Research Center,  
Yorktown Heights, NY 10598, USA*

(Dated: March 23, 2022)

## Abstract

We investigate generalized soliton-bearing systems in the presence of external perturbations. We show the possibility of the transport of solitons using external waves, provided the waveform and its velocity satisfy certain conditions. We also investigate the stabilization and transport of bubbles using external perturbations in 3D-systems. We also present the results of real experiments with laser-induced vapor bubbles in liquids.

PACS numbers: 05.45.Yv Solitons, 42.65.-k Nonlinear optics, 47.55.Dz Drops and bubbles

---

\* E-mail: jorge@ivic.ve

† E-mail: leo@ivic.ve

## I. INTRODUCTION

Recently, in a very interesting paper, Zheng *et al.*, [1] have studied the collective directed transport of symmetrically coupled lattices in symmetric periodic potentials. They show that under the action of an external wave, that breaks the spatiotemporal symmetry and introduces inhomogeneities of the lattice, a net unidirectional current can be observed. Apparently the current originates from the collaboration of the lattice and the wave (amplitude, frequency, and phase shifts). The study of directed transport of particles is very important in the physics of molecular motors [2, 3], vortex dynamics in superconductors [4, 5], Josephson junction lattices [6], nanotechnology [7, 8] and many other systems.

Many studies have been dedicated to directed transport in spatiotemporal systems [9, 10, 11, 12, 13, 14, 15, 16, 17, 18]. These include systems with deterministic ac drives and stochastic forces [13, 14, 15, 16, 17, 18].

Very important are models composed of a symmetrically coupled lattice in a symmetric potential field, which is driven by an external wave [1].

The equation studied by Zheng *et al.*, [1] is the following:

$$\dot{\theta}_j = -d \sin \theta_j + \kappa (\theta_{j+1} - 2\theta_j + \theta_{j-1}) + A \cos(\omega t + j\phi). \quad (1)$$

This is a Frenkel–Kontorova model driven by the wave  $A \cos(\omega t + j\phi)$ .

The average current introduced by them  $J = \lim_{T \rightarrow \infty} \sum_{j=1}^N \int_0^T \dot{\theta}_j(t) dt$  was shown to be nonzero for certain values of the parameters of the system.

We wish to re-state this problem in terms of the directed motion of solitons. Solitons are considered as particles in many systems. Moreover, in many systems, the solitons are charge carriers [19, 20, 21, 22, 23]. So it is very important to study the directed transport of these objects.

In the present paper we investigate the generalized Klein–Gordon equation:

$$\phi_{tt} + \gamma \phi_t - \phi_{xx} - G(\phi) = F(x - wt), \quad (2)$$

where  $G(\phi) = -\partial U(\phi)/\partial \phi$ ,  $U(\phi)$  is a symmetric potential with, at least, two minima at  $\phi = \phi_1$ ,  $\phi = \phi_3$ , and a maximum at  $\phi = \phi_2$  ( $\phi_1 < \phi_2 < \phi_3$ );  $F(x - wt)$  describes an external wave moving with velocity  $w$ . Both the sine–Gordon and  $\phi^4$  equations are particular cases of equation (2). The sine–Gordon equation is a continuous relative of Eq. (1).

These equations possess important applications in condensed matter physics. For instance, in solid state physics, they describe domain walls in ferromagnets and ferroelectric materials, dislocations in crystals, charge-density waves, interphase boundaries in metal alloys, fluxons in long Josephson junctions and Josephson transmission lines, etc [24, 25, 26].

Our initial condition will be a kink-soliton whose center-of-mass is situated at rest in the point  $x = 0$ . We will show that the transport of the soliton by the wave depends on the shape of the wave and the parameters of the system.

We will also investigate the stabilization and transport of bubbles using external perturbations in 3D-systems as the following

$$\phi_t - \nabla^2 \phi - G(\phi) = F(x, y, z, t). \quad (3)$$

We will also present the results of real experiments with laser-induced bubbles in liquids.

The bubbles can be trapped, stabilized and transported by a laser beam of relatively low power. We will show that the directed transport of solitons and bubbles are related. For both phenomena some conditions for the external perturbations must be satisfied.

## II. STABILITY AND DYNAMICS OF SOLITONS

Before discussing equation (2) we would like to present some results about the dynamics of solitons in the presence of time-independent inhomogeneous perturbations [27, 28, 29, 30, 31, 32] as in the following equation:

$$\phi_{tt} + \gamma \phi_t - \phi_{xx} - G(\phi) = F(x). \quad (4)$$

Suppose we are interested in the stability of a soliton situated in equilibrium positions created by the inhomogeneous force  $F(x)$ . We construct a solution  $\phi_k(x)$  with the topological and general properties of a kink. Then, we solve an inverse problem such that  $F(x)$  possesses the properties of the physical system we are studying [27, 28, 29, 30, 31, 32]. Now we can investigate the stability of the solution.

For this we should solve the spectral problem

$$\hat{L}f(x) = \Gamma f(x), \quad (5)$$

where  $\hat{L} = -\partial_{xx} - \frac{\partial G(\phi)}{\partial \phi} \Big|_{\phi=\phi_k(x)}$ ,  $\phi(x, t) = \phi_k(x) + f(x)e^{\lambda t}$ ,  $\Gamma = -(\lambda^2 + \gamma\lambda)$ .

The results obtained with this function can be generalized qualitatively to other systems topologically equivalent to the exactly solvable systems [27, 33].

Let us see the following example:

$$\phi_{tt} + \gamma\phi_t - \phi_{xx} + \sin\phi = F_1(x), \quad (6)$$

where  $F_1(x) = 2(B^2 - 1) \sinh(Bx) / \cosh^2(Bx)$ .

The exact stationary solution of Eq. (6) is  $\phi_k(x) = 4 \arctan[\exp(Bx)]$ . This solution represents a kink-soliton equilibrated on the position  $x = 0$ . The stability problem (5) can be solved exactly. The eigenvalues of the discrete spectrum are given by the formula

$$\Gamma_n = B^2(\Lambda + 2\Lambda n - n^2) - 1, \quad (7)$$

where  $\Lambda(\Lambda + 1) = 2/B^2$ . The integer part of  $\Lambda$ , i.e.,  $[\Lambda]$ , yields the number of eigenvalues in the discrete spectrum, which correspond to the soliton modes (this includes the translational mode  $\Gamma_0$ , and the internal or shape modes  $\Gamma_n$  ( $n > 0$ )).

Everything that happens with this solution near point  $x = 0$  can be obtained from Eq. (7).

Now let us return to the general case (4) and a review of the obtained results about the dynamics of solitons in Eq. (4).

Wherever  $F(x)$  is positive, the kink-soliton will be accelerated to the “left”. Wherever  $F(x)$  is negative, the kink-soliton will be accelerated to the “right”. The zeroes of  $F(x)$  are candidates for equilibrium positions for the kink-soliton [27, 28, 29, 30, 31, 32]. If  $F(x)$  possesses only one zero  $x_0^*$  ( $F(x_0^*) = 0$ ), then it is a stable position for the soliton if  $\frac{\partial F}{\partial x}|_{x_0^*} > 0$ . Otherwise, the position is an unstable equilibrium. The opposite is true for the antikink-soliton. A soliton can be trapped by a  $F(x)$  with a zero that represents a stable position, and it can move away from an unstable position.

Now we will discuss what happens in the Eq. (2) with different waveforms.

### III. TRANSPORT OF SOLITONS USING EXTERNAL PERTURBATIONS

Fig. 1 shows different waveforms for  $F(x - vt)$ . In case a) the kink will move trapped inside the potential well created by  $F(x - vt)$ . The effective potential  $V(x)$  of this force  $F(x)$  possesses the property that  $V(x) \rightarrow \infty$  when  $x \rightarrow \pm\infty$ . Thus, the kink will move inside a potential equivalent to a harmonic oscillator. So a wave like this will always transport the soliton to the “right”.

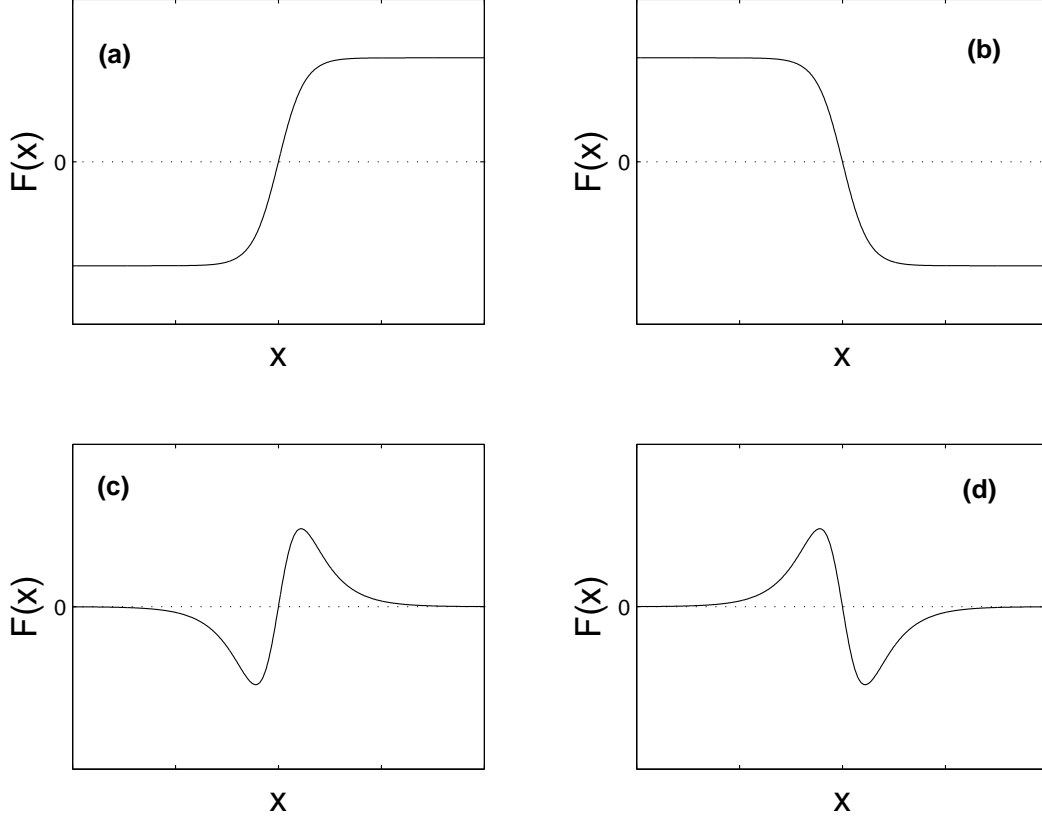


FIG. 1: Different waveforms for the transport of solitons in Eq. (2). a) The soliton feels a moving deep stable potential well. b) The soliton feels an unstable equilibrium position. c) The soliton feels a potential well with finite walls. d) The soliton feels a potential with a finite maximum.

In the case b), the wave will “push” the soliton to the “right” as long as the center-of-mass of the soliton is situated righter than the zero of  $F(x)$ . In fact,  $V(x)$  has an absolute maximum. However, there is a limit for the wave velocity. If the wave velocity exceeds this limit, the center-of-mass of the soliton can reach the maximum of the potential  $V(x)$ , and the center-of-mass of the soliton will be behind the maximum of the potential. In this situation the wave can no longer push the soliton to the “right”.

We will here introduce the concept of “controlled transport” when the soliton can be transported by the external wave and the soliton velocity can be approximately equal to the wave velocity. In the case a) of Fig. 1, we have a controlled transport. In the case b), the soliton is pushed by the wave but the soliton will move ahead of the wave in an “uncontrolled” fashion.

The waveform shown in Fig. 1 c represents a force that creates a stable equilibrium for the

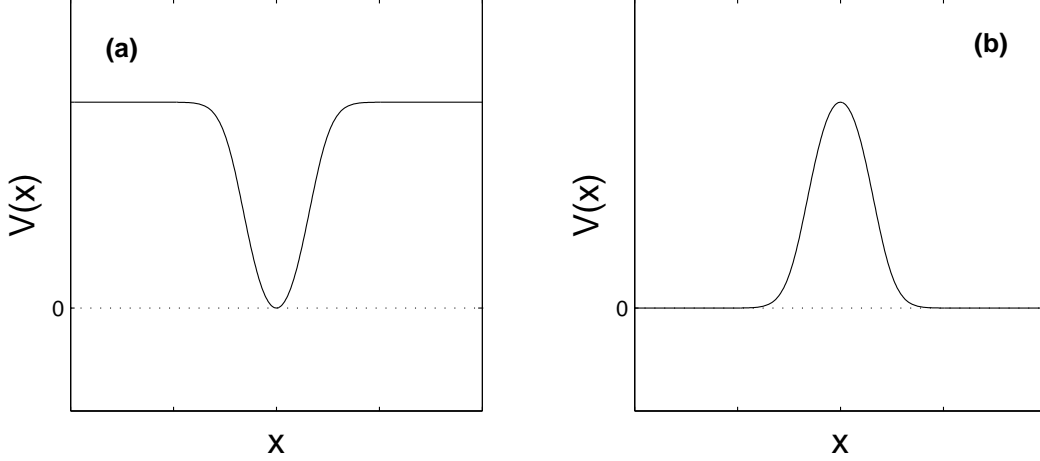


FIG. 2: Effective potential “created” by the forces shown in Fig. 1 (c) and (d) respectively.

soliton. So, as in case a), this wave can carry the soliton. However, the effective potential corresponding to this force is finite for  $x \rightarrow \pm\infty$  (See Fig. 2 a).

So here there is also a limit for the wave velocity.

The wave represented in Fig. 1 d is an unstable equilibrium for the soliton as in case b). This wave can push the soliton to the “right” provided its velocity is smaller than certain finite value.

Fig. 3 shows some different localized wave forms.

We would think that these waves could also be used to transport a soliton in a controlled fashion because there is a stable equilibrium involved (provided the wave velocity is smaller than certain limit). However, here there are some additional limitations in the shape of the wave.

Investigating different functions in (4) and the stability problem (5), we have found that if  $F(x)$  possesses several zeroes and the distance between them is smaller than the soliton width, surprising phenomena can occur. For instance, in the presence of forces as that shown in Fig. 3 a, if the zeroes of  $F(x)$  are too close, the center zero is not a stable point anymore. In practice, the soliton does not “feel” a minimum there. It feels an unstable equilibrium point. In this case, this wave would not be able to transport the soliton in a controlled fashion, but it can push the soliton to the right under certain conditions.

On the other hand, the force shown in Fig. 3 c can carry the soliton if the zeroes are sufficiently separated. Otherwise, the soliton would not “feel” the left maximum of the potential  $V(x)$  (Fig. 3 d). So, using this wave the soliton cannot move trapped in the

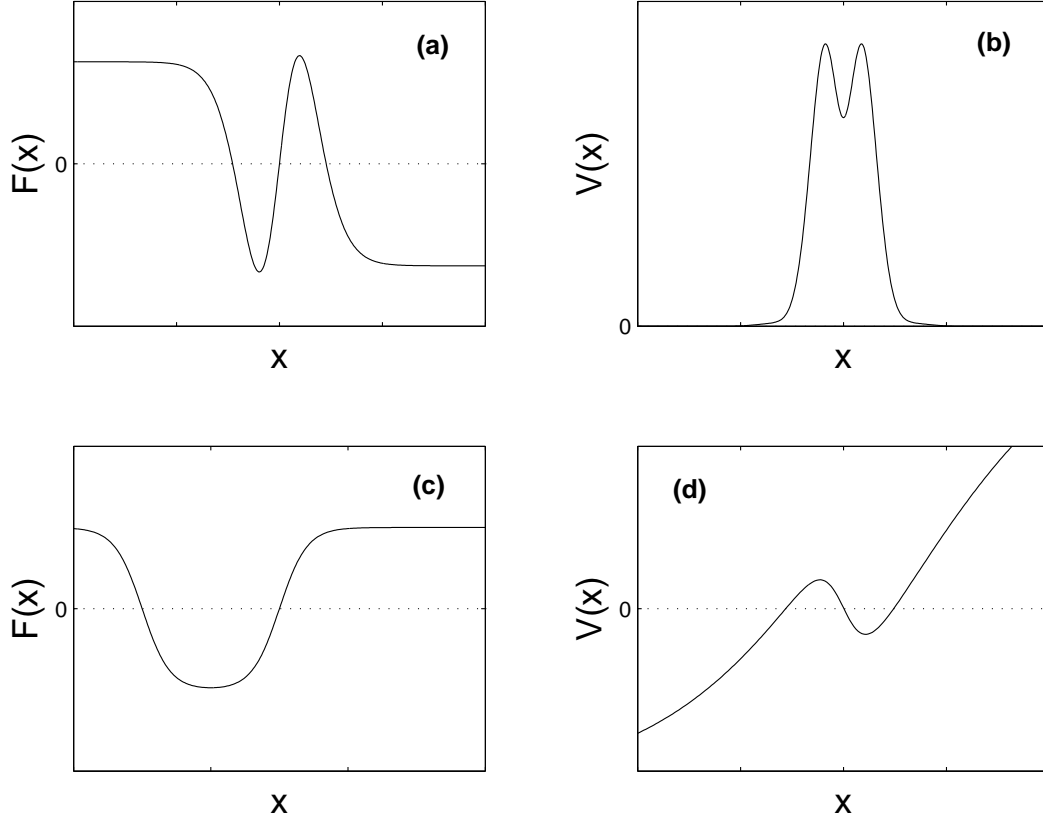


FIG. 3: Perturbation with several zeroes.

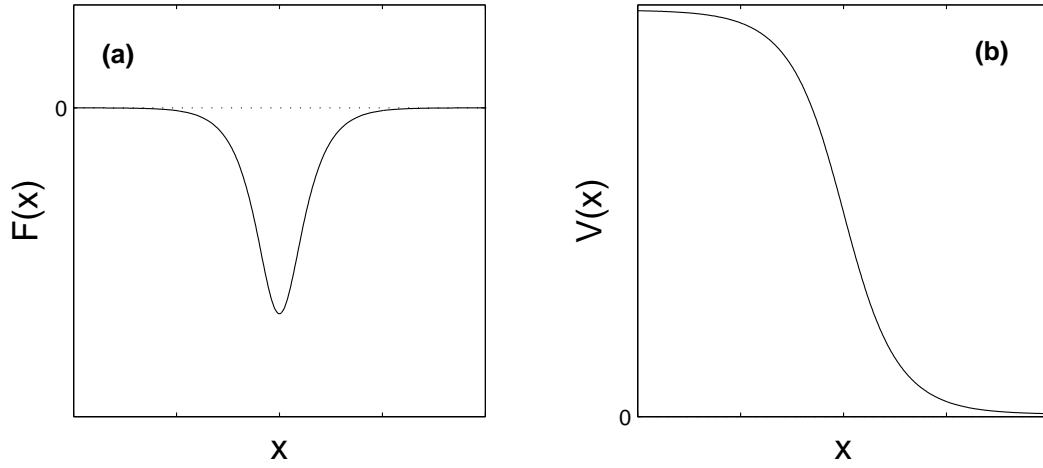


FIG. 4: Perturbation equivalent to a wall.

minimum.

Even localized forces without a zero like that represented in Fig. 4 can “push” the soliton to the “right”.

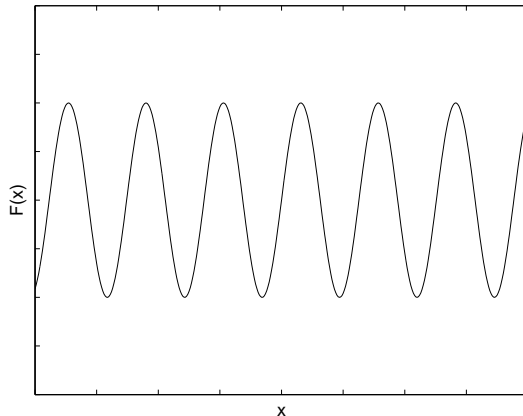


FIG. 5: Sinusoidal wave.

Note that, considering the effective potential  $V(x)$ , this wave “acts” on the soliton as a moving “wall”. But once and again, there is a limit for the velocity of the wave.

Later we will present several examples of systems of type (2) for which we can calculate all these limit velocities.

Before, we should discuss the most ubiquitous kind of waves: the sinusoidal wave (See Fig. 5):

$$F(x - wt) = A \sin[k(x - wt)]. \quad (8)$$

The previous discussion of waves with the shape shown in Fig. 3 leads us to think that the parameters  $A$ ,  $k$  and  $w$  should satisfy some conditions for a soliton to be transported by wave (8). In fact, if the velocity  $w$  is larger than some critical value, the soliton will be left behind. If  $k$  is too large (and  $A$  is small), the distance between the zeroes of  $F(x)$  will be very small and the potential wells, where the soliton can be trapped, would be so shallow that, already with certain small velocity  $w$ , the soliton will be left behind. Thus there are waves of type (8) that cannot carry the soliton.

Let us present here some concrete examples.

Consider the following perturbed  $\phi^4$  equation:

$$\phi_{tt} + \gamma\phi_t - \phi_{xx} - \frac{1}{2}\phi + \frac{1}{2}\phi^3 = F(x - wt), \quad (9)$$

where  $F(x - wt) = A \tanh[B(x - wt)]$ ,  $A > 0$ ,  $B > 0$ . As can be expected from our discussion, this external wave is able to transport a soliton to the right in a controlled fashion. This can be observed in Fig. 6.



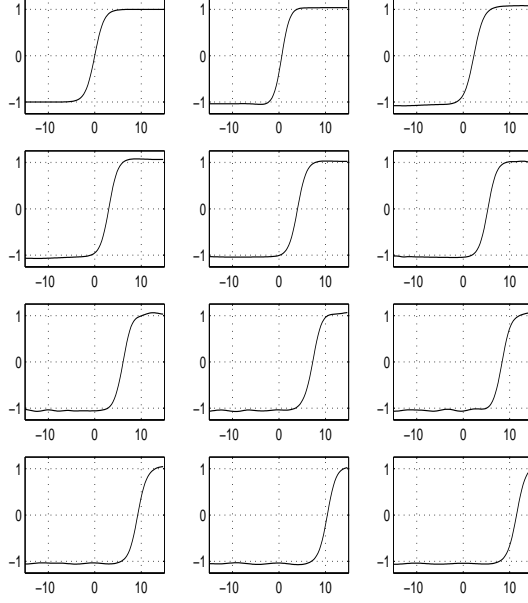


FIG. 6: The soliton is transported by the moving perturbation  $F(x - wt) = A \tanh[B(x - wt)]$  (See Eq. (9)).

Later we will see that  $F(x - wt)$  can be in practice not only a wave but a controlling external perturbation. If this external perturbation can be manipulated at wish in such a way that the velocity  $w(t)$  can be any function of time that we desire, then we can move the soliton and place it wherever we wish.

Suppose now that in Eq. (9)  $F(x - wt) = -A \tanh[B(x - wt)]$ ,  $A > 0$ ,  $B > 0$ . In this case, the soliton is pushed to the “right” while it is in the “zone” where  $F(x - wt) < 0$  (i.e., while the center-of-mass of the soliton is situated righter than the zero of  $F(x - wt)$ .) Let us define  $\phi_1 < \phi_2 < \phi_3$  as the roots of the algebraic equation  $\phi - \phi^3 = 2A$ . The maximum velocity  $v_m$  that the solution can reach in its motion to the right [28] can be calculated using the equation

$$\frac{\gamma v_m}{\sqrt{1 - v_m^2}} = \frac{\phi_2}{2} \quad (10)$$

If the external wave velocity is such that  $w > v_m$ , then the soliton eventually will start to move backward.

Now we will analyze the following wave  $F(y)$ , where  $y = x - wt$ :

$$F(y) = F_1(y), \quad \text{for } y > y^* \quad (11)$$

$$F(y) = c, \quad \text{for } y < y^* \quad (12)$$

where  $F_1(y) = \frac{1}{2}A \tanh(By)[(A^2 - 1) + (4B^2 - A^2)\text{sech}^2(By)]$ ,  $y_*$  is the point where  $F_1(y)$  has a local maximum; and  $c = F_1(y_*)$ .

This problem is equivalent to that shown in Fig. 3 c and 3 d provided  $A^2 > 1$ ,  $4B^2 < 1$ . The effective potential possesses a local minimum and a local maximum at the left side of the minimum.

Using the results of papers [28, 29] we can solve exactly the dynamical problem of the soliton in this potential.

Our analysis shows that if  $2B^2(3A^2 - 1) < 1$ , then the soliton feels the barrier in the point  $y = 0$ . So, if the wave velocity  $w$  is small, the soliton can be carried to the right. On the other hand, if  $2B^2(3A^2 - 1) > 1$  (although the waveform is still as that shown in Fig. 3 c such that  $F(y)$  has two zeroes), the soliton will move to the left, crossing the barrier even if its center-of-mass is placed in the minimum of the potential and its initial velocity is zero. The soliton does not feel the barrier. Even with an infinitesimal wave velocity, the soliton will not move to the right dragged by the wave. We have checked this phenomenon numerically.

The effect of a wave shaped as that in Fig. 4 can be seen in the following example with exact solution:

$$\phi_{tt} + \gamma\phi_t - \phi_{xx} - \frac{1}{2}\phi + \frac{1}{2}\phi^3 = \frac{A}{\cosh^2 \left[ \frac{1}{2} \left( \frac{x-wt}{\sqrt{1-w^2}} \right) \right]}. \quad (13)$$

When  $A = -\frac{\gamma}{2} \frac{w}{\sqrt{1-w^2}}$ , the following travelling soliton is an exact solution  $\phi = \tanh \left[ \frac{1}{2} \left( \frac{x-wt}{\sqrt{1-w^2}} \right) \right]$ . Note that a wave shaped like that in Fig. 4 can make the soliton move to the right. However, for a fixed  $A$  in Eq. (13), the wave velocity should not exceed a limit. Otherwise, the soliton can be left behind.

In the case of a sinusoidal wave acting in the framework of the  $\phi^4$  equation:

$$\phi_{tt} + \gamma\phi_t - \phi_{xx} - \frac{1}{2}\phi + \frac{1}{2}\phi^3 = A \sin [k(x - wt)], \quad (14)$$

we can write the following conditions for the soliton to be dragged by the wave to the right:  $\frac{\pi}{k} > 4$ ,  $w < v_m$ , where  $v_m$  is defined by the equation  $\frac{\gamma v_m}{\sqrt{1-v_m^2}} = \frac{\phi_2}{2}$ , and  $\phi_2$  is the “middle” root to the algebraic equation  $\phi - \phi^3 = 2A$  as in Eq. (7).

We have experimented with other waveforms that illustrate the different behaviors discussed above.

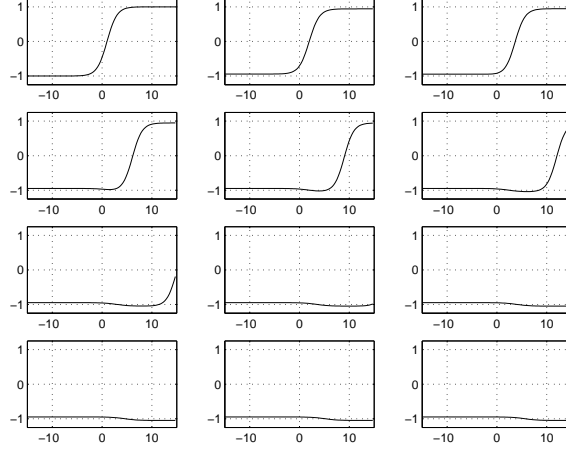


FIG. 7: A kink-soliton can be pushed by unstable equilibrium.  $F(x, t) = a \tanh[B(x - wt)]$ ,  $\phi(x, 0) = 2B \tanh[B(x - x_0)]$ ,  $\phi_t(x, 0) = 0$ ,  $B = 0.5$ ,  $w = 0.05$ ,  $a = -0.05$ ,  $x_0 = 1.0$ ,  $\gamma = 0.5$

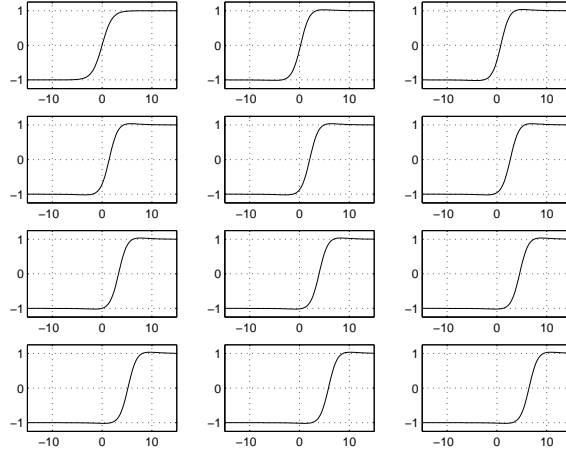


FIG. 8: The soliton is transported by the perturbation:  $F(x, t) = a \sinh[B(x - wt)] / \cosh^3[B(x - wt)]$ ,  $\phi(x, 0) = 2B \tanh(Bx)$ ,  $\phi_t(x, 0) = 0$ ,  $B = 0.5$ ,  $w = 0.1$ ,  $a = 0.2$ ,  $\gamma = 0.5$

The force  $F(x, t) = a \tanh[B(x - wt)]$ , with  $a < 0$  has the properties of the function shown in Fig. 1b.

Fig. 7 shows that the soliton can be pushed by this external perturbation, provided the velocity  $w$  is not too large.

In Fig. 8 we present the behavior of the soliton under the action of the external perturbation  $F(x, t) = \frac{a \sinh[B(x - wt)]}{\cosh^3[B(x - wt)]}$ , which is of the kind shown in Fig. 1c.

When  $w = 0.1$ , the soliton is transported in a controlled way by the external wave.

However, already when  $w = 0.5$ , the soliton is abandoned behind. This can be observed

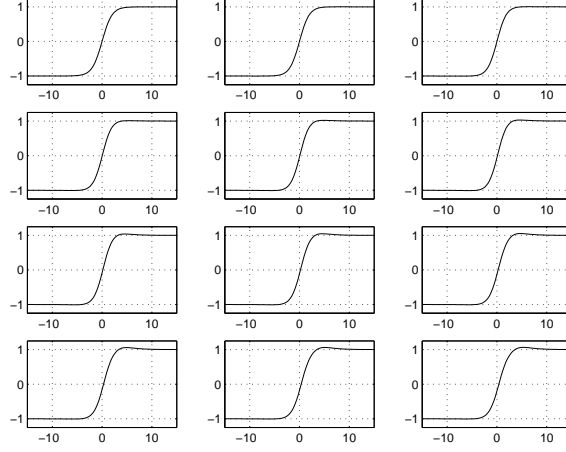


FIG. 9: The same experiment as in Fig. 8. However, the wave velocity is larger, and the soliton is not transported by the wave. ( $F(x, t) = a \sinh[B(x-wt)] / \cosh^3[B(x-wt)]$ ,  $\phi(x, 0) = 2B \tanh(Bx)$ ,  $\phi_t(x, 0) = 0$ ,  $B = 0.5$ ,  $w = 0.5$ ,  $a = 0.2$ ,  $\gamma = 2.0$ )

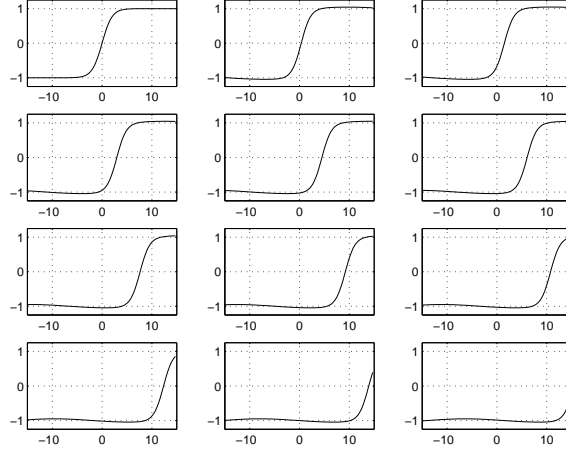


FIG. 10: A periodic wave can carry the soliton. ( $F(x, t) = A \sin[\kappa x - wt]$ ,  $\phi(x, 0) = 2B \tanh(Bx)$ ,  $\phi_t(x, 0) = 0$ ,  $B = 0.5$ ,  $w = 0.01$ ,  $A = 0.05$ ,  $\kappa = 0.2$ ,  $\gamma = 0.5$ )

in Fig. 9.

A periodic wave like  $F(x, t) = A \sin[kx - wt]$  is able to carry the soliton as is shown in Fig. 10 where  $w = 0.01$ . The values of the other parameter can be found in the figure caption of Fig. 10.

If the wave velocity is too large (say  $w = 0.9$ ), then the soliton cannot be carried by the external wave (See Fig. 11).

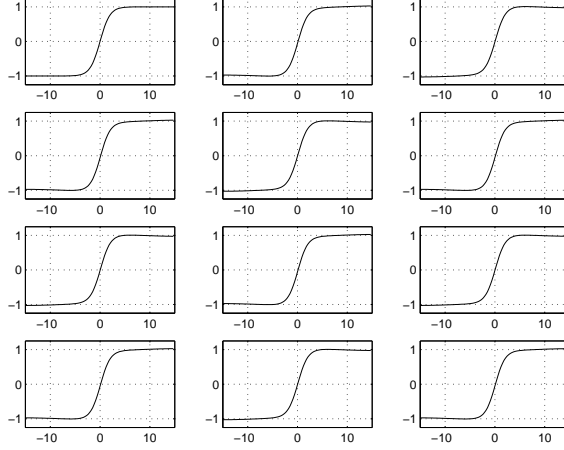


FIG. 11: The periodic wave must satisfy some combinations in order to transport the soliton. In this case, for a larger wave velocity, the soliton is left behind. ( $F(x, t) = A \sin[\kappa x - wt]$ ,  $\phi(x, 0) = 2B \tanh(Bx)$ ,  $\phi_t(x, 0) = 0$ ,  $B = 0.5$ ,  $w = 0.9$ ,  $A = 0.05$ ,  $\kappa = 0.2$   $\gamma = 0.5$ )

#### IV. BUBBLES IN SOLITON EQUATIONS

Phase transitions [33, 34, 35, 36, 37, 38, 39, 40, 41, 42, 43, 44] can be described by an equation similar to (2):

$$\phi_{tt} + \gamma \phi_t - \nabla^2 \phi = -\frac{\partial U(\phi)}{\partial \phi} + F(x, y, z, t). \quad (15)$$

Recall that  $U(\phi)$  possesses two minima ( $\phi_1$  and  $\phi_3$ ) and a maximum ( $\phi_1 < \phi_2 < \phi_3$ ).

Suppose for the moment that  $U(\phi_1) < U(\phi_3)$ . The main phenomenon for  $F \equiv 0$  is that of “nucleation” where drops or bubbles grow or disappear depending on their Gibbs energies [33, 34, 35, 36, 37, 38, 39, 40, 41, 42, 43, 44].

The relevant issue is the transition from the metastable state  $\phi_3$  to the state  $\phi_1$ . In phase-transition theory, researchers consider the existence of a critical “germ” for the transition. Field configurations  $\phi(\mathbf{x}, t)$  with a “radius” larger than that of the critical germ should grow in order to produce the transition to the state  $\phi_1$ .

Let us first discuss this situation in the context of the one-dimensional equation

$$\phi_{tt} + \gamma \phi_t - \phi_{xx} = -\frac{\partial U(\phi)}{\partial \phi}. \quad (16)$$

For  $U(\phi_1) < U(\phi_3)$ , it is possible to show (see Refs. [33] and [45]) that there exists an unstable stationary critical solution that plays the role of a critical germ. This solution is represented in Fig. 12.

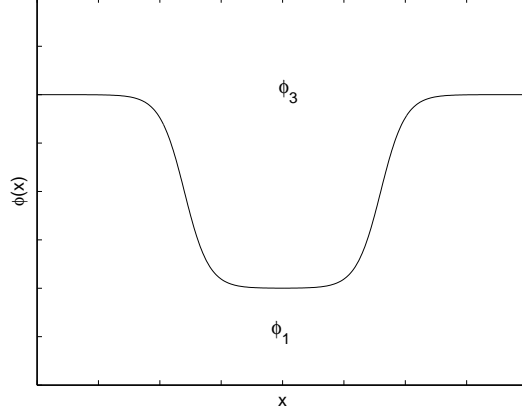


FIG. 12: A “bubble” formed by a kink–antikink pair in Eq. (17)

This solution can be interpreted as a kink–antikink pair [45, 46].

In general, a kink and an antikink attract each other [46, 47]. On the other hand, a constant external force acts on a kink and an antikink in different directions. So the solution represented in Fig. 12 is possible when the kink and the antikink are at some critical distance where the attraction force and the external force balance each other [46, 47].

The critical solution is unstable [33, 46]. Perturbations of the critical solution can lead to the growth of the critical “bubble” initiating the transition to the state  $\phi = \phi_1$ . “Bubbles” with a radius smaller than the radius of the critical solution will disappear, whereas “bubbles” with a radius larger than the radius of the critical solution will grow until the whole system is in the state  $\phi = \phi_1$ .

An example can be studied in the equation

$$\phi_{tt} + \gamma\phi_t - \phi_{xx} - \frac{1}{2}\phi + \frac{1}{2}\phi^3 = F_0, \quad (17)$$

where  $F_0 = \text{const.}$

Note that Eq. (17) can be written in the form (16), where

$$U(\phi) = \frac{1}{8}(\phi^2 - 1)^2 - F_0\phi. \quad (18)$$

If  $F_0 < 0$ , then  $U(\phi_1) < U(\phi_3)$ . Eq. (17) possesses a bell-shaped stationary solution as that shown in Fig. 12. This solution is unstable [45, 46]. Similar but different bell-shaped initial states will evolve either to the state  $\phi = \phi_1$  or the state  $\phi = \phi_3$ . If the kink and the antikink that form the one-dimensional “bubble” are too close, then the bubble will

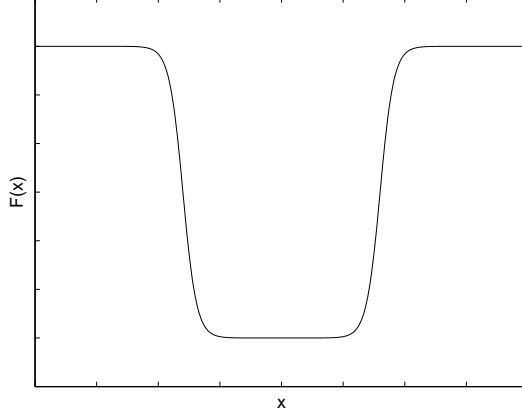


FIG. 13: Inhomogeneous external perturbation able to stabilize the bubble in Eq. (19)

collapse. If the distance between the kink and the antikink is larger than the “width” of the critical germ, then the “bubble” will grow.

If  $F_0 = 0$ , all the initial bubbles will collapse.

Can we stabilize the bubbles of phase  $\phi = \phi_1$  inside the “sea” of phase  $\phi = \phi_3$  using external perturbations?

Let us analyze what happens when a kink–antikink pair as that shown in Fig. 12 is in the presence of an external perturbation like that shown in Fig. 13

Note that these graphs look similar but they represent very different physical quantities.

If the kink of Fig. 12 is close to the “right” zero of function  $F(x)$ , it will “feel” an effective potential well (see Fig. 14). The same will happen to the antikink if it is close to the “left” zero of  $F(x)$  in Fig. 13 (See the potential in Fig. (15).)

If the potential barrier is sufficiently high, the attraction force between the kink and the antikink will not lead to the “bubble” collapse. The attraction force decays rapidly (exponentially) with the distance, so for large “bubbles” practically “any”  $F(x)$  with the shape of Fig. 13 is good for stabilizing the “bubble”.

On the other hand, even small bubbles can be stabilized using an external perturbation  $F(x)$  with two zeroes  $x_1$  and  $x_2$  (as in Fig. 13) such that  $\left| \left( \frac{dF(x)}{dx} \right)_{x=x_{1,2}} \right|$  is sufficiently large. That is, the change of sign in  $F(x)$  should be sufficiently sharp.

We have checked numerically the existence of the stable “bubbles”.

Let us experiment with the following equation

$$\phi_{tt} + \gamma\phi_t - \phi_{xx} - \frac{1}{2}\phi + \frac{1}{2}\phi^3 = F(x), \quad (19)$$

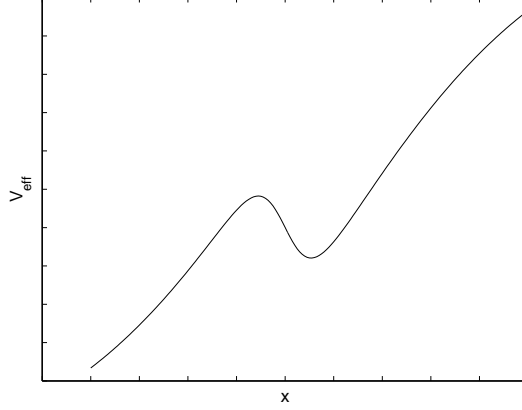


FIG. 14: Effective potential for the kink that forms the “bubble” shown in Fig. (12) in the presence of perturbation shown in Fig. (13)

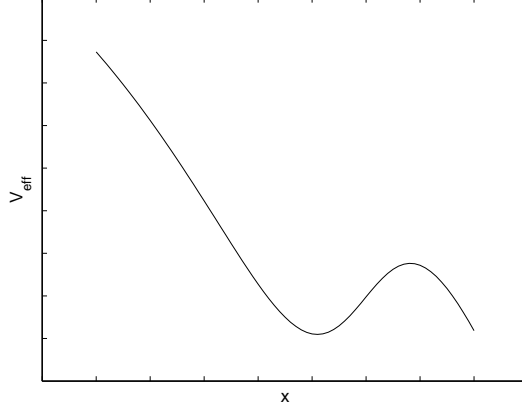


FIG. 15: Effective potential for the antikink that forms the “bubbles” shown in Fig. (12) in the presence of perturbation shown in Fig. (13)

where

$$F(x) = A \{ \tanh [B(x - d)] - \tanh [B(x + d)] + \epsilon \} \quad (20)$$

For instance, we have established that the perturbations (20), with the parameters  $A = 1$ ,  $B = 0.2$ ,  $d = 5$ ,  $\epsilon = 0.7$ , can sustain a stable bubble.

An initial configuration for  $\phi(x, t)$  where the kink and the antikink are not exactly in the zeroes of  $F(x)$  will, anyway, tend to the asymptotically stable bubble. That is, there is a bubble which is a spatiotemporal attractor. All close initial configurations will tend (for  $t \rightarrow \infty$ ), to the asymptotically stable bubble.

This phenomenon occurs in the case that a bubble is considered as an initial configuration. That is, a bubble had been created before the “force”  $F(x)$  is applied. However, it is



interesting to remark that for sufficiently large  $A$  and  $B$ , the perturbation itself can create the bubble. That is, there is no need for a preexisting bubble. The bubble is created by the perturbations and, then, the perturbation can sustain the stabilized bubble.

If  $A$  is too small, it is possible that  $F(x)$  cannot sustain a bubble. An example is produced with the following parameters  $A = 0.25$ ,  $B = 1.0$ ,  $d = 1.0$ ,  $\epsilon = 0.8$ . All initial conditions lead to the bubble collapse.

Once we have an external perturbation  $F(x)$  able to sustain a stable bubble, we can transport the bubble if we can move  $F(x)$  as a whole. This phenomenon is in the same spirit of all the theory discussed above concerning the soliton transport.

In the case of the bubble, as in many of the discussed situations with solitons, there is a limit for the velocity of the perturbation as a whole. When the shape represented in Fig. 13 is moved too fast, the bubble can be left behind, and then it will collapse.

## V. THREE DIMENSIONAL BUBBLES

What about the bubbles in three dimensions?

Let us concentrate on solutions with radial symmetry.

The stationary solutions of Eq. (15) ( $F(x, y, z, t) \equiv 0$ ), satisfy the equation

$$\phi_{rr} + \frac{2}{r}\phi_r - \frac{\partial U(\phi)}{\partial \phi} = 0. \quad (21)$$

It is possible to prove [33] that (for  $U(\phi_1) < U(\phi_3)$ ) there exists a solution with a minimum in  $r = 0$  and that asymptotically it tends to  $\phi_3$  as  $r \rightarrow \infty$ . This solution corresponds to the critical germ discussed above. Again as before, this critical solution is unstable.

In general, exact solutions for the three-dimensional case of the nonlinear equation (21) are very difficult to find [33]. Nevertheless, we have developed an inverse-problem approach that allows us to find exact solutions to a class of topologically equivalent systems.

For instance, a wealth of work [33] has been dedicated to find a solution to equations of type

$$\phi_{rr} + \frac{2}{r}\phi_r - B^2\phi + D^2\phi^3 + T(\phi) = 0, \quad (22)$$

where  $T(\phi)$  possesses only terms of higher order than 3. This equation is important in field theory.

We have found that function

$$\phi = \frac{A \tanh(Br)}{r \cosh(Br)} \quad (23)$$

is the exact solution to equation  $\phi_{rr} + \frac{2}{r}\phi_r - B^2\phi + \frac{1}{A^2}\phi^3 + T(\phi) = 0$ , where  $T(\phi)$  contains only terms of order higher than 3.

Likewise, it can be proved that function

$$\phi = \phi_3 - \frac{A \tanh(Br)}{r \cosh(Br + D)} \quad (24)$$

is the critical germ solution of an equation of type (21), where  $U(\phi)$  possesses all the properties that we need: two minima and a maximum,  $U(\phi_1) < U(\phi_3)$ , etc.

As in the one-dimensional case, small bubbles will collapse, and bubbles with a radius larger than that of the critical germ will grow.

In the context of the three-dimensional equation:

$$\phi_{tt} + \gamma\phi_t - \nabla^2\phi - \frac{1}{2}\phi + \frac{1}{2}\phi^3 = 0, \quad (25)$$

all the bubbles are non-stationary. However, we should say that very large bubbles are quasi-stationary because the interaction between the walls is so small that (although they should collapse eventually) their life-time is very large.

What about inhomogeneous perturbations as in Eq.(15)?

Suppose we have an initial configuration  $\phi(\mathbf{x}, t = 0)$  with the shape of a spherical bubble of phase  $\phi = \phi_1$  inside a “sea” of phase  $\phi_3$ . This means that there is a spherical spatial sector where  $\phi \approx \phi_1$ , and, outside this sector,  $\phi \approx \phi_3$ . Space zones where  $F(x, y, z) < 0$  will “try” to expand the bubble. Space zones where  $F(x, y, z) \geq 0$  will “try” to make the bubble collapse.

In fact, as in the one-dimensional case, we can stabilize a spherical bubble using an inhomogeneous external perturbation  $F(x, y, z)$  such that  $F(x, y, z) < 0$  for points  $(x, y, z)$  that are inside the bubble and  $F(x, y, z) > 0$  for points  $(x, y, z)$  outside the bubble.

To ensure the stability of the bubble, the sign change of  $F(x, y, z)$  should be sharp. We have an exact solution.

Let us define the equation

$$\phi_{tt} + \gamma\phi_t - \nabla^2\phi - \frac{1}{2}\phi + \frac{1}{2}\phi^3 = F(r), \quad (26)$$

where

$$\begin{aligned}
F(r) = & \frac{1}{2}A(A^2 - 1) \left\{ \tanh \left[ \frac{A}{2}(r - R) \right] \right. \\
& \left. - \tanh \left[ \frac{A}{2}(r + R) \right] \right\} \\
& + \frac{3}{2} \{ (\phi_1 + \phi_2) [\phi_1\phi_2 + A(\phi_1 + \phi_2) + A^2] \} \\
& - \frac{2}{r} [\phi_{1r} + \phi_{2r}] - \frac{1}{2}A + \frac{1}{2}A^3,
\end{aligned}$$

$r = \sqrt{x^2 + y^2 + z^2}$ ,  $\phi_1 = A \tanh [B(r - R)]$ ,  $\phi_2 = -A \tanh [B(r + R)]$ ;  $A$ ,  $B$  and  $R$  are real parameters.

Here  $F(r)$  has the desired property that  $F(r) < 0$  in a spherical sector around  $r = 0$ , and  $F(r) > 0$  outside this spherical sector.

There is an exact bubble solution to Eq. (26):

$$\phi = A \left\{ \tanh \left[ \frac{A}{2}(r - R) \right] - \tanh \left[ \frac{A}{2}(r + R) \right] + 1 \right\}. \quad (27)$$

But we can say more. For  $R > 5$ ,  $A > 1$ , this bubble solution is stable. Manipulating  $F(r)$  we can control this bubble. In fact, we can move this bubble to another point in space.

## VI. BUBBLES IN PHASE TRANSITIONS

Many works have been dedicated to the nucleation process in phase transitions [33, 34, 35, 36, 37, 38, 39, 40, 41, 42, 43, 44, 45]. Here we wish to focus on the works based on the theory of relaxation of metastable states [42, 43, 44].

In Refs.[42, 43, 44], the nucleation in the metastable phase near the critical point of a thermodynamic system is described as a relaxation of a metastable state of the order-parameter field.

A metastable state of matter can be produced in a first-order phase transition. Its relaxation into a thermodynamically stable state is facilitated by the formation of a critical nucleus of a new phase.

The system is described by a scalar field  $\phi(\mathbf{x}, t)$  for which a relaxation equation is obtained:

$$\frac{1}{\Gamma_n} \frac{\partial \phi}{\partial t} = -\frac{\delta H}{\delta \phi} + f_{ext}, \quad (28)$$

where  $H[\phi]$  is the system free-energy which is taken in the Landau form:

$$H[\phi] = \frac{1}{2} \int \left\{ c (\nabla \phi)^2 + \mu \phi^2 + \frac{1}{2} g \phi^4 - 2h\phi \right\} d\mathbf{x}. \quad (29)$$

Here  $\Gamma_n$  is a kinetic coefficient and  $f_{ext}$  is an external perturbation.

At  $h = 0$  and  $\mu = \mu_c < 0$ , there is a critical point in the system. The line  $h = 0$  ( $\mu < \mu_c$ ) is a line of first-order phase transition.

The Eq. (28) is an overdamped version of the  $\phi^4$  equation discussed above. This equation can be written in dimensionless units as our equations (2). The solution we have been investigating describes a nucleus of phase  $\langle \phi \rangle = -1$  in phase  $\langle \phi \rangle = 1$ . At  $h < 0$ , the nuclei with small radius attenuate, while the nuclei with large radius increase. The phase  $\langle \phi \rangle = 1$  at  $h < 0$  is metastable-unstable to formation of a nucleus with a large radius.

The parameters of the system (28–29) for the liquid–vapor first-order phase transition depend on the thermodynamics quantities, e.g., pressure and temperature [43, 44].

If an external perturbation (say a laser beam) creates the thermodynamics conditions for a first-order transition (e.g.,  $h < h_c < 0$  in the context of system (28–29)) in a small zone of a liquid mass, then a vapor bubble could be generated and sustained.

We should say here that in the framework of equation

$$\gamma \phi_t - \nabla^2 \phi - \frac{1}{2} \phi + \frac{1}{2} \phi^3 = F(x, y, z), \quad (30)$$

in order to create a bubble able to increase to a macroscopic radius,  $F(x, y, z)$  must take negative values in a limited spatial zone in such a way that  $F(x, y, z) < -\frac{1}{3\sqrt{3}}$ . On the other hand, once the bubble has been generated, the perturbation  $F(x, y, z)$  necessary to sustain the bubble should be “negative” inside the bubble and positive “outside”, but the absolute value of  $F(x, y, z)$  in the “negative” part should not be so high. In other words, the “intensity” of the perturbation needed for generating the bubble is larger than the needed “intensity” for stabilizing the bubble.

## VII. REAL EXPERIMENTS: BUBBLES INDUCED AND CONTROLLED BY LASERS

Now we will discuss several experiments about bubble formation in a weak absorbing liquid and its subsequent trapping under the action of a cw laser beam of relatively low power.

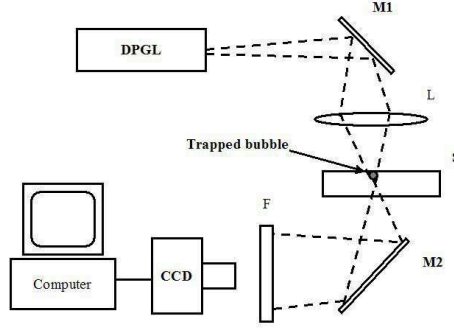


FIG. 16: Experimental Setup

The generation of bubbles by intense light pulses was studied in the papers [48, 49]. On the other hand, the pioneering works about laser bubble trapping can be found in Refs. [50, 51]. Here we present a review of previous [48, 49] and very recent experiments concerning new effects related to laser bubble trapping, in the light of the theory we are developing.

High-intensity light induces a local first-order liquid-vapor phase transition. If light power is reduced after the bubble formation, the bubble remains trapped. If the intensity is very low then the bubble collapses.

The experimental setup is shown in Fig. 16.

In Figure 16 we show the experimental set-up used for the laser bubble generation and subsequent trapping. A CW 200 mW diode pumped green laser ( $\lambda=532$  nm) is directed vertically down toward a horizontally located sample cell using the mirror M1. A 15-cm focal length lens L focuses this light onto the sample. By moving this lens we can change the radius of the focal spot. The sample is a 4-mm thick glass cell containing an iodine ethanol solution of high concentration (1 to 10 ml). The focused beam heats this solution, generating locally a small bubble at power levels larger than 60 mW. Following the light absorption a distribution of temperatures is induced in the focal region and the bubble surface. Because the surface tension depends upon the temperature, a spatial distribution of surface tension is generated on the bubble. The generated gradient of surface tension induces a force that traps the bubble at the point of maximal temperature (focal point). This generated force together with the floatation Archimedes force make the bubble sticks to the upper surface of the cell. By moving the laser beam using the mirror M1, the bubble follows the beam spot demonstrating the actual bubble trapping by the laser beam. The

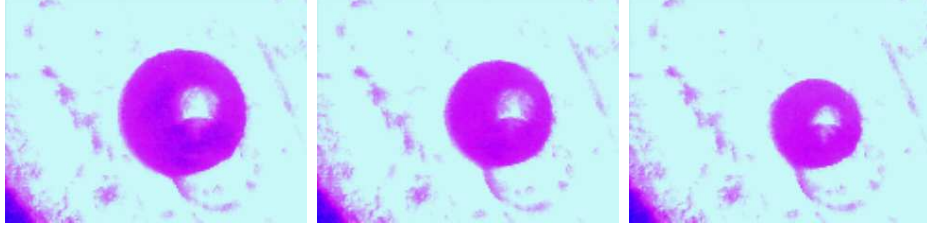


FIG. 17: Trapped bubble using a laser. The laser power is 1.7 mW (left), 0.5 mW (center) and 0.15 mW (right). The bubble's diameters depend on the laser power.

bubble can be observed using the mirror M2 and a CCD camera connected to a computer.

The used liquids were ethanol, benzene, and ethylene glycol. The liquids were colored with iodine or a dye in order to increase absorption.

We will focus here on the bubble behavior. There are several interference phenomena that will not be discussed here.

In Fig. 17–19 pictures of the trapped bubbles are shown.

In one of the experiments the bubble is generated at a laser power of 70 mW. The bubble size decreases with decreasing power.

These phenomena can be described in terms of thermal gradients and forces [51]. However, we wish to stress the universal character of the phenomena related to bubble formation and transport. These effects can occur in many other physical systems with phase transitions, solitons, domain walls and bubbles of one phase inside other phase,

The bubble can be controlled by the laser.

If after creating the bubble, the light beam is defocused in such a way that its spot size becomes much larger than the radius of the generated bubble, then changes of the bubble radius occur until this radius is again stabilized. This can be explained using the interpretation discussed above where the bubble is described as trapped inside a stable equilibrium position or potential well.

The bubbles are created with a laser power of 70 mW. Then the power is decreased about 10 times.

In Fig. 17 we can observe a trapped bubble with a diameter 0.4 mm using a laser power 1.7 mW. When the laser power is 0.15 mW the bubble diameter is 0.2 mm.

Fig. 18 shows the transport of the bubble using the laser beam. With the help of a mirror the light beam is moved. The trapped bubble can be moved as the light beam is moved

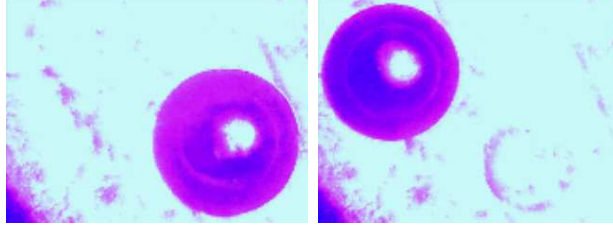


FIG. 18: Transport of the bubble: (left) The bubble is shown at its initial position. (right) The bubble is moved to the left superior corner

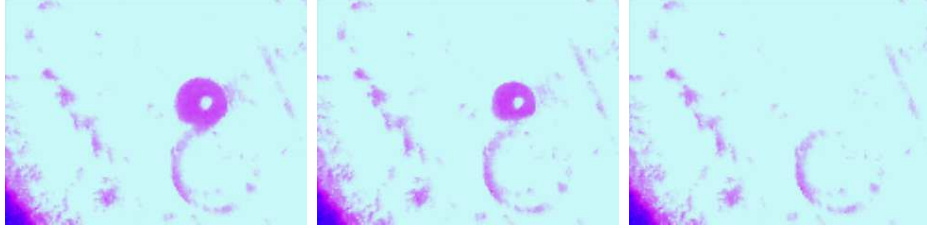


FIG. 19: The bubble can collapse when the laser power is small.

slowly. If the motion of the light beam is too fast, then the bubble is left behind and then it collapses.

In Fig. 18 (left), the bubble is shown at its initial position. Then it is moved to the left superior corner using the laser beam.

Fig. 19 shows the collapse of the bubble while the light power is maintained in 0.1 mW.

## VIII. CONCLUSIONS

We have investigated generalized nonlinear Klein–Gordon equations perturbed by moving inhomogeneous external perturbations.

We have shown that a kink–soliton can be transported by an external wave, provided the shape of the wave and its velocity satisfy certain conditions. For instance, a moving external perturbation  $F(x - vt)$ , where function  $F(y)$  possesses a zero  $y_0$  such that  $\frac{\partial F}{\partial y}\big|_{y=y_0} > 0$ , can carry a kink–soliton provided its velocity does not exceed certain limit. Figures 1, 3 and 5 show examples of these transporting inhomogeneous perturbations. Sinusoidal waves as that shown in Fig. 5 can also be successful in transporting a kink–soliton under certain conditions.

We have also determined the necessary conditions to be satisfied by an external pertur-

bation to stabilize a bubble of one phase inside another.

If this stabilizing inhomogeneous external perturbation is moved, then the bubble can be transported to another space point.

We have presented the results of real experiments with laser-induced vapor bubbles in liquids. The bubbles can be created, trapped, stabilized and transported by a laser beam of relatively low power.

The investigated equations are very general. Besides, the concepts and results that lead to the existence of the reported phenomena are also universal. So we believe that these phenomena can be observed in many other physical systems. For instance, the stabilization and transport of bubbles using an external perturbation can occur in other systems undergoing a phase-transition. So the mentioned bubbles (or drops) can be superconducting, ferromagnetic, superfluid, etc.

On the other hand, the discussed transport of solitons and kink-antikink bubbles can be very important in spin systems, molecular motors, charge-density waves, ferroelectric materials and Josephson junctions. In particular, in long Josephson junctions the kink-solitons are fluxons. These fluxons can be controlled using external currents [26, 31] which can be very relevant in new communication and computer technologies where the fluxons are used as very stable information units.

Moreover, the kinks are examples of topological defects. Many results about the kinks can be generalized to other topological defects as vortices and spiral waves which are being studied intensively in countless systems nowadays [52, 53, 54, 55].

- 
- [1] Z. Zheng, M. C. Cross and G. Hu, Phys. Rev. Lett. **89**, 154102 (2002).
  - [2] R. D. Astumian, Science **276**, 917 (1997).
  - [3] F. Julicher *et al.*, Rev. Mod. Phys. **69**, 1269 (1997).
  - [4] C. S. Lee *et al.*, Nature **400**, 337 (1999).
  - [5] C. J. Olson *et al.*, Phys. Rev. Lett. **87**, 177002 (2001).
  - [6] E. Trias *et al.*, Phys. Rev. E **61**, 2257 (2000).
  - [7] J. Rousselet *et al.*, Nature **370**, 446 (1994).
  - [8] A. V. Oudenaarden *et al.*, Science **285**, 1046 (1999).



- [9] P. Reimann, Phys. Rep. **361**, 57 (2002).
- [10] I. Derenyi and T. Vicsek, Phys. Rev. Lett. **75**, 374 (1995).
- [11] Z. Csahok *et al.*, Phys. Rev. E **55**, 5179 (1997).
- [12] A. Igarashi *et al.*, Phys. Rev. E **64**, 051908 (2001).
- [13] Z. Zheng *et al.*, Phys. Rev. Lett. **86**, 2273 (2001).
- [14] Z. Zheng and X. Li, Commun. Theor. Phys. **36**, 151 (2001).
- [15] P. Jung *et al.*, Phys. Rev. Lett. **76**, 3436 (1996).
- [16] J. L. Mateos, Phys. Rev. Lett. **84**, 258 (2000).
- [17] S. Flach *et al.*, Phys. Rev. Lett. **84**, 2358 (2000).
- [18] O. Yevtushenko *et al.*, Europhys. Lett. **54**, 141 (2001).
- [19] S. A. Gredeksul and Y. S. Kivshar, Phys. Rep. **216**, 1 (1992).
- [20] A. J. Heeger, S. Kirelson, J. R. Schrieffer and W. -P. Su, Rev. Mod. Phys. **60**, 781 (1988).
- [21] A. S. Davidov, *Solitons in Molecular Systems* (Naukova Dumka, Kiev, 1984).
- [22] M. A. Rice, Phys. Lett. A **71**, 152 (1979), *ibid* **73**, 153 (1979).
- [23] Y. Lu, *Solitons and Polarons in Conducting Polymers* (World Scientific, Singapore, 1988).
- [24] *Solitons in Action*, edited by K. Lonngren and A. C. Scott (Academic, London, 1978).
- [25] A. R. bishop, J. A. Krumhanst and S. E. Trullinger, Physica D **1**, 1 (1980).
- [26] Yu. S. Kivshar and B. A. Malomed, Rev. Mod. Phys. **61**, 763 (1989).
- [27] J. A. González, B. A. Mello, L. I. Reyes and L. E. Guerrero, Phys. Rev. Lett. **80** 1361 (1998).
- [28] J. A. González and J. A. Holyst, Phys. Rev. B **45** 10338 (1992).
- [29] J. A. González and B. A. Mello, Phys. Lett. A **219** 226 (1996).
- [30] J. A. González, L. E. Guerrero and A. Bellorín, Phys. Rev. E **54** 1265 (1996).
- [31] J. A. González, A. Bellorín and L. E. Guerrero, Phys. Rev. E **60** R37 (1999).
- [32] J. A. González, A. Bellorín and L. E. Guerrero, Phys. Rev. E **65** 065601(R) (2002).
- [33] J. A. González and F. A. Oliveira, Phys. Rev. B **59**, 6100 (1999).
- [34] J. S. Langer, Ann. Phys. (N.Y.) **41**, 108 (1967).
- [35] M. Büttiker and R. Landauer, Phys. Rev. A **23**, 1397 (1981).
- [36] J. S. Aubry, J. Chem. Phys. **62**, 3217 (1975).
- [37] S. Coleman, Phys. Rev. D **15**, 2929 (1977); *ibid.* **16**, 1248(E) (1977).
- [38] C. G. Callan and S. Coleman, Phys. Rev. D **16**, 1762 (1977).
- [39] M. A. Collins, A. Blumen, J. F. Currie and J. Ross, Phys. Rev. B **19**, 3630 (1979)

- [40] D. A. Gorukhov and G. Blatter, Phys. Rev. B **58**, 5486 (1998).
- [41] A. E. Filippov, Yu. E. Kuzovlev and T. K. Sobolova, Phys. Lett. A **165**, 159 (1992).
- [42] A. Z. Patashinskii and B. I. Shumilo, Sov. Phys. JETP **50**, 712 (1979).
- [43] A. Z. Patashinskii and V. L. Pokrovskii, *Fluctuation theory of phase transitions* (Navka, Moscow, 1975).
- [44] A. Z. Patashinskii, *Statistical description of metastable states* Preprint INP 78–44, Novosibirsk, 1978 (unpublished).
- [45] J. A. González and J. A. Holyst, Phys. Rev. B **35** 3643 (1987).
- [46] J. A. González and J. Estrada–Sarlabous, Phys. Lett. A **140** 189 (1989).
- [47] B. A. Mello, J. A. González, L. E. Guerrero and E. López–Atencio, Phys. Lett. A **244** 277 (1998).
- [48] W. Lauterborn, Acustica **31**, 51 (1974).
- [49] P. Giovanneschi and D. Dufresne, J. App. Phys. **58**, 651 (1985).
- [50] A. Marcano, App. Opt. **31**, 2757 (1992).
- [51] A. Marcano and L. Aranguren, App. Phys. B **56**, 343 (1995).
- [52] M. C. Cross and P. C. Hehenberg, Rev. Mod. Phys. **65**, 851 (1993).
- [53] I. S. Aranson and L. Kramer, Rev. Mod. Phys. **74**, 99 (2002).
- [54] M. Bär and M. Or–Guil, Phys. Rev. Lett. **82**, 1160 (1999).
- [55] L. Q. Zhou and Q. Ouyang, Phys. Rev. Lett. **85**, 1650 (2000).